

# INTERNAL STRUCTURE OF HYPERON CONFIGURATIONS OF STELLAR MASSES

V. A. Ambartsumyan and G. S. Saakyan

Byurakan Astrophysical Observatory, Academy of Sciences, ArmSSR  
 Translated from *Astronomicheskii Zhurnal*, Vol. 38, No. 6,  
 pp. 1016-1024, November-December, 1961  
 Original article submitted January 25, 1961

The internal structure of equilibrium configurations of stellar masses possessing a density of the order of the density of the atomic nucleus and higher was studied. It is shown that the space metric inside the configurations deviates markedly from the Euclidean metric. In addition, the total number of baryons in the configurations discussed in our previous contribution [1] was calculated. For large values (of the total number of baryons), there are two solutions with different total energies. Of these, the configurations considered to be wholly stable are those associated with a larger mass defect.

## 1. Structure of Configurations Consisting of an Ideal Baryonic Gas

In our previous contribution [1], where we considered several equations of state, we derived values of some of the important parameters specifying superdense configurations consisting of a degenerate baryonic gas. In performing numerical calculations, we obtained all the necessary parameters specifying the internal structure of the configurations as a matter of course. Below, we consider in somewhat greater detail the structure of the configurations calculated under the assumption of an ideal Fermi gas.

Figure 1 shows curves characterizing the variation of the parameter  $t_n(r)$  inside the star for four configurations corresponding to different values of  $t_n(0)$ . As we readily see in recalling the previous article [1], the density is found as a function of  $t_n(r)$ , so that these curves offer a graphic picture of the density distribution of the intrastellar matter.

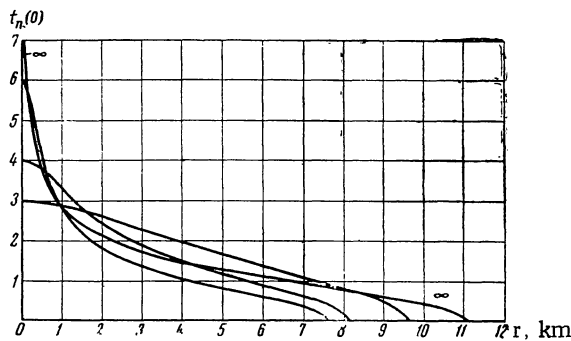


Fig. 1. Parameter  $t_n(r)$  as a function of the coordinate  $r$ . Distances are given in kilometers. The definition of  $t_n$  may be found by reference to our earlier paper ([1], Eq. (1.2)).

Figure 2 shows curves of  $U(r)$  for six different ideal gas states. These configurations differ in values of  $t_n(0)$  plotted on each curve.

The curve plotted for  $t_n(0) = 1$  does not terminate within the confines of the graph. It actually extends out to  $r = 21.1$  km.

We are in a position to also calculate the components of the metric tensor  $g_{rr}(r)$  and  $g_{00}(r)$  on the basis of the results obtained.

For  $g_{rr}(r)$  in the interior of the star, we have [2]:

$$\frac{1}{g_{rr}(r)} = e^{-\lambda(r)} = 1 - \frac{2u(r)}{r}, \tag{1.1}$$

and in the space outside the star:

$$\frac{1}{g_{rr}(r)} = 1 - \frac{2M}{r}; \quad r > R, \tag{1.2}$$

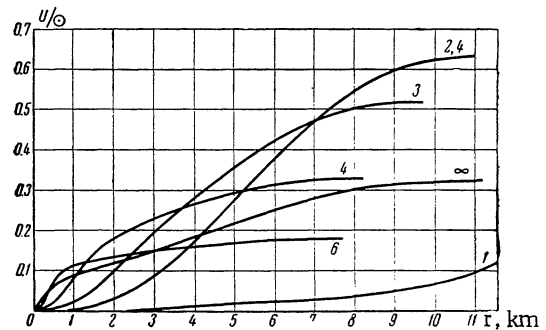


Fig. 2. Graph of function  $U(r)$ . Distances are measured in kilometers. The numbers on the curves denote values of the parameter  $t_n(0)$ . The curve for  $t_n(0) = 1$  extends out to  $r = 21.1$  km.  $U(r)$  gives an approximate idea of the mass concentrated in a sphere of radius  $r$ .  $U$  values are in solar mass units.

where  $M$  is the stellar mass and  $R$  is the stellar radius. The last formula is the familiar outer Schwarzschild solution.

The dependence of component  $g_{rr}$  of the metric tensor on the magnitude of the radius vector for five different configurations is plotted in Fig. 3. The numbers attached to the curves denote the value of parameter  $t_n(0)$ . We see that the metric deviates quite decidedly from the Euclidean metric. Theories of superdense configurations resting on the Newtonian gravitational theory as a basis would therefore incur sizable errors.

The time component  $g_{00}$  of the metric tensor outside the configurational volume is determined by the formula

$$-g_{00}(r) = \frac{1}{g_{rr}(r)} = 1 - \frac{2M}{r}; \quad r > R. \quad (1.3)$$

Inside the configurational volume, however, the value of  $g_{00}$  may be arrived at on accepting the starting point that the matter exists in a state of thermodynamic and mechanical equilibrium. The equilibrium conditions for the neutronic component are of the form [3]

$$\sqrt{-g_{00}(r)} \mu_n(r) = \sqrt{-g_{00}(R)} \mu_n(R) = \text{const}, \quad (1.4)$$

where  $\mu_n(r)$  is the chemical potential of the neutron gas at a distance  $r$  from the center of the configuration.

Since we are discussing a highly degenerate state, the chemical potential of the gas is equal to the critical Fermi energy for the gas particles

$$\mu_n(r) = c [m_n^2 c^2 + p_n^2(r)]^{1/2}. \quad (1.5)$$

Formula (1.4) is valid, strictly speaking, only for the region containing neutrons. In practice, however, neutrons appear at only a slight depth from the stellar surface in all our configurations. The outer layer consisting wholly of protons and electrons is quite tenuous. Neglecting this layer, then, we may write  $p_n(R) = 0$  and  $\mu_n(R) = m_n c^2$ . With this in mind, and not overlooking Eqs. (1.3) and (1.4), we find the following from Eq. (1.4) for  $g_{00}$ :

$$-g_{00}(r) = \left(1 - \frac{2M}{R}\right) \cosh^2 \frac{t_n(r)}{4}. \quad (1.6)$$

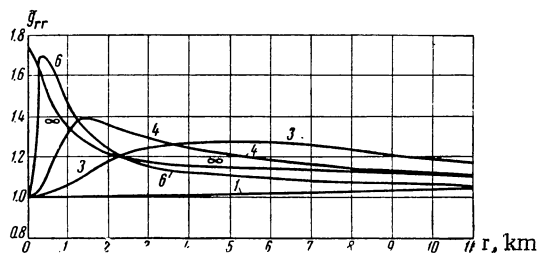


Fig. 3. Dependence of component  $g_{rr}$  of metric tensor on  $r$ . As  $r \rightarrow \infty$ , the function  $g_{rr}$  tends to its Euclidean value of unity.  $r$  is measured in kilometers.

Curves  $t_n(r)$  are plotted in Fig. 1. At  $r \geq R$ , we have  $t_n(r) = 0$  and Eq. (1.6) goes over into Eq. (1.3).

The function  $g_{00}(r)$  is graphed for some values in Fig. 4. The numbers attached to the curves indicate the value of  $t_n(0)$  for the configuration in question. The  $g_{00}(r)$  is interesting for the configuration where the density at the center, and consequently  $t_n(0)$  as well, goes to infinity. In this case,  $g_{00}(0)$  vanishes and the four-dimensional interval transforms to a purely spatial interval. From the standpoint of an external observer, the phenomena occurring at the center of that configuration must proceed at an infinitely slow rate.

Note that the metric properties of three-dimensional space are specified by the tensor  $\gamma_{\alpha\beta} = g_{\alpha\beta} - g_{0\alpha} g_{0\beta} / g_{00}$ , where  $\alpha, \beta = 1, 2, 3$ . In our case, however, (i.e., a static field), this tensor contains only the diagonal elements  $g_{0\alpha} = 0$  and  $\gamma_{rr} = g_{rr}$ .

We shall not cite the corresponding data characterizing the inner structure of the configurations consisting of a real gas. For obvious reasons, the non-Euclidean nature of space in this case is more strongly pronounced in the volume of the configurations and in the adjacent regions.

In our preceding contribution [1], the term radius was taken to mean the value of the coordinate  $r$  at the surface of the star. The actual stellar radius  $R_0$  is found from the formula:

$$R_0 = \int_0^R \sqrt{g_{rr}} dr; \quad (1.7)$$

and its value differs markedly from the coordinate radius  $R$  for the configurations discussed here. Numerical values of  $R_0$  are given in Table 1.

## 2. Number of Baryons in Star

The material presented in the preceding paragraphs furnishes us with grounds for asserting that all the para-

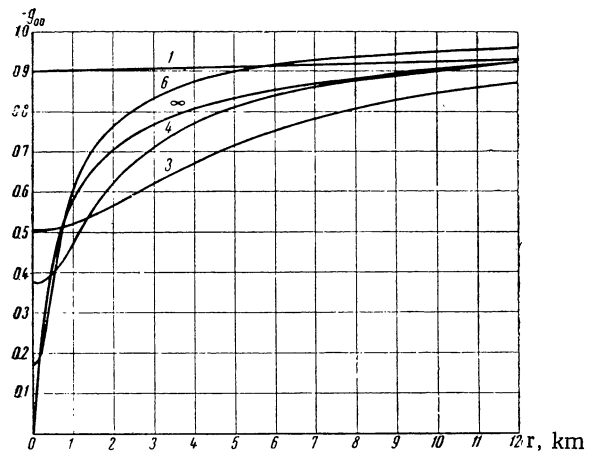


Fig. 4. Dependence of time component  $g_{00}(r)$  of metric tensor.  $g_{00} = 1$  corresponds to Euclidean space.

TABLE 1. Dependence of Number of Baryons, Radius, and Packing Fractions  $\alpha_1$  and  $\alpha_2$  on the Parameter  $t_n(0)$

Ideal gas						Real gas					
$t_n(0)$	number of baryons, $\underline{n} \cdot 10^{56}$	radius, km		$10^2 \cdot \alpha_1$	$10^2 \cdot \alpha_2$	$t_n(0)$	number of baryons, $\underline{n} \cdot 10^{56}$	radius, km		$10^2 \cdot \alpha_1$	$10^2 \cdot \alpha_2$
		of star	of hyperon core					of star	of hyperon core		
0.556	1.70	—	—	4.9	0.558	2.1	9.33	13.0	—	9.3	7.32
1.0	4.03	—	—	10.0	1.80	2.2	9.75	12.7	2.91	7.4	10.0
1.3	5.34	18.7	—	8.7	2.68	2.4	11.0	11.2	4.9	7.1	14.5
1.5	6.07	16.3	—	9.0	3.92	2.6	13.1	9.53	5.81	7.7	28.5
1.8	7.23	15.2	—	8.5	5.52	3.0	12.7	6.90	5.66	3.9	39.9
2.4	8.00	11.8	3.37	5.8	8.76	3.1	11.5	6.97	5.68	2.3	45.0
2.75	7.30	11.1	3.74	6.0	9.87	3.2	9.8	6.81	5.33	-2.7	47.2
3.0	6.56	10.4	3.49	6.0	10.4	3.3	8.22	6.69	5.34	-12	48.8
3.3	5.52	9.98	3.28	3.2	10.9	3.4	6.55	6.56	5.00	-22	54.6
4.0	4.01	9.12	2.79	2.4	12.9	3.8	6.72	6.98	5.09	-18	55.6
5.0	2.48	7.48	2.13	-9.1	15.9	4.0	6.83	7.15	5.29	-16	55.2
6.0	1.96	8.24	1.83	-7.3	19.8	5.0	7.00	7.11	5.32	-16	54.5
7.0	2.46	11.1	1.67	-6.3	15.4	7.0	7.00	7.21	5.32	-16	54.5
$\infty$	3.70	11.1	2.31	-3.8	10.9	$\infty$	7.03	7.19	5.30	-16	54.8

meters specifying stable superdense configurations constitute a single-valued function of the central density of matter, represented by the parameter  $t_n(0)$ . On the other hand, we see that the converse assertion is not always correct. And indeed, in some range of values of one or the other observable parameter (e.g., mass or radius), two or even three widely divergent values of density of matter at the center may correspond to one single value of that parameter (cf. Figs. 1 and 2 in our preceding contribution [1]).

The study of the relationship between stellar parameters and the number of baryons in the star, and the dependence of that number on the density value at the center are problems of heightened interest. The number of baryons in a star, denoted  $\underline{n}$  in what follows, is derived from the formula

$$n = 4\pi \int_0^R \sqrt{g_{rr}} N(r) r^2 dr, \quad (2.1)$$

where  $N(r) = \sum_k N_k(r)$  is the total baryon density at a distance  $r$  from the center.

The integral (2.1) was computed for various configurations of ideal and real gases. To achieve this, we had to first plot curves of  $N(r)$ . The results of the calculations appear in the second and eighth columns of Table 1.

We must dwell for a moment on the configurations with infinitely large density at the center. In this case we can derive an asymptotic expression for the number of baryons enclosed within a central sphere of rather small radius  $r_c$ .

In order to arrive at an asymptotic formula for  $n(r)$ , note that at  $t_n \gg 1$ , we have  $\sinh t_k \approx 9 \cosh^4(t_n/4)$ . Moreover, from the conditions for equilibrium states (cf. Eqs. (1.4) and (1.5) from [1]), we find that

$$m_k \cosh(t_k/4) \approx m_n \cosh(t_n/4) \quad (2.2)$$

(in the case of central particles the equation will be an identity). Bearing in mind Eq. (2.2) for baryon density, we find

$$N = \frac{32}{3} \frac{K_n}{m_n c^2} \sum_k \frac{1}{2} a_k \left( \frac{m_k}{m_n} \sinh \frac{t_k}{4} \right)^3 \approx \frac{32 K_n s}{3 m_n c^2} \cosh^3 \frac{t_n}{4}, \quad (2.3)$$

where  $s = \sum_k a_k/2 = 11$ .

In the case of an ideal gas, we have for the density of matter

$$\rho = K_n \sum_k \frac{1}{2} a_k \left( \frac{m_k}{m_n} \right)^4 (\sinh t_k - t_k) + m_n c^2 N_n \approx 8s K_n \cosh^4(t_n/4). \quad (2.4)$$

Comparison of Eqs. (2.3) and (2.4) yields

$$N(r) \approx \frac{32}{3 \cdot 8^{3/4}} \frac{(s K_n)^{3/4}}{m_n c^2} \rho^{3/4}(r). \quad (2.5)$$

Hence, taking into account the asymptotic solution (4.4) derived in [1]:

$$N(r) \approx \sigma r^{-3/2}, \quad (2.6)$$

where

$$\sigma = 3.86 \frac{K_n^{3/4}}{m_n c^2} \left( \frac{c^4}{4\pi k} \right)^{3/4}.$$

For regions of space where the asymptotic solution is applicable,  $g_{rr}$  has the constant value  $g_{rr} \approx 7/4$ .

Substitution of Eq. (2.6) into (2.1) yields

$$n(r) = 4\pi \int_0^r \sqrt{g_{rr}} N(r) r^2 dr \approx 7.83 \cdot 10^{48} r^{3/2}. \quad (2.7)$$

It was shown in our previous contribution [1] that the asymptotic solution is an excellent one out to distances slightly in excess of  $r \approx 10^8$  cm. This value of  $r$  yields us  $n = 2.28 \cdot 10^{53}$  baryons from Eq. (2.7). The number of baryons present in the remainder of the star was obtained subsequently by numerical integration. As a result, the number of varyons was found to be  $3.7 \cdot 10^{56}$  for the configuration  $t_n(0) = \infty$ .

Let us now proceed to a derivation of an asymptotic expression for  $n(r)$  in the case of a real gas. In this case, as  $t_n \rightarrow \infty$

$$\rho = K_n \sum_k \frac{1}{2} a_k \left( \frac{m_k}{m_n} \right)^4 (\sinh t_k - t_k) + m_\pi c^2 N_\pi + NU(N) \approx NU(N).$$

For the model of a real gas considered here (cf. Eq. (5.1) in [1]), we find

$$\rho \approx 3.2 \cdot 10^{-83} N^3. \tag{2.8}$$

Adopting the asymptotic solution (5.6) derived in [1], we find:

$$N(r) \approx 1.94 \cdot 10^{27} \left( \frac{c^4}{4\pi k} \right)^{1/3} r^{-2/3}. \tag{2.9}$$

Within the domain of applicability of the asymptotic solution,  $g_{rr} = 17/9$ . From Eq. (2.1), and taking Eq. (2.9) into account, we obtain

$$n(r) \approx 1.42 \cdot 10^{44} r^{7/3}. \tag{2.10}$$

We saw that the asymptotic solution was a good one out to distances  $r \approx 300$  cm. From Eq. (2.10), we find  $n(r) = 6.94 \cdot 10^{49}$  for the number of baryons within the sphere indicated. Starting at distance  $r = 274$  cm, the number of varyons for configuration  $t_n(0) = \infty$  was computed by means of numerical integration. This yields the result  $n = 7 \cdot 10^{56}$  particles.

Curves of mass of calculated configurations vs. total number of baryons present are plotted in Fig. 5. The solid curve refers to the case where the equation for a "real" Fermi gas comes into play. The dashed curve represents the case of an ideal Fermi gas. Values of the parameter  $t_n(0)$  at the center of the configuration in question are plotted at several points of the curve for clarification. At  $t_n(0) < 1.8$  the curves coincide. Only one solid-line curve need be drawn for this region, representing both the case of a real and that of an ideal gas. It is clear from inspection of the graph that  $M(n)$  is single-valued for a real gas over the range  $n < 6.5 \cdot 10^{56}$ , ... double-valued in the range  $7.1 \cdot 10^{56} < n < 13.5 \cdot 10^{56}$  and triple-valued in the intermediate region  $6.5 \cdot 10^{56} < n < 7.1 \cdot 10^{56}$ . In the case of ideal-gas models, the function  $M(n)$  is single-valued at  $n < 2 \cdot 10^{56}$ , double-valued at  $3 \cdot 10^{56} < n < 8.1 \cdot 10^{56}$ , and triple-valued in the intermediate range  $2 \cdot 10^{56} < n < 3 \cdot 10^{56}$ .

Models of an ideal gas corresponding to points on the lower branch of the graph are purely neutronic

models. Points on the upper branch correspond to hyperon configurations. In the case of a real gas, hyperon configurations are found on both branches, but states corresponding to upper-branch points contain a still higher percentage of hyperons.

This fact that, starting from some value of  $n$  (equal to  $6.5 \cdot 10^{56}$  in the case of a real gas) there correspond to each  $n$  two or three equilibrium configurations, is a very important fact. It is obvious that of the two (or three) equilibrium configurations corresponding to a specified  $n$ , that configuration of lesser mass will be the more stable. Inspection of the accompanying graph shows that a configuration of large mass exhibits a high density at the center. It would seem that the high density at the center must signify a large gravitational mass defect, in consequence of which the total mass of the configuration must be smaller in this case. However, a high configurational mass is actually arrived at, because the percentage of hyperons having large intrinsic masses is considerable.

It is evident that a star located on the upper branch of the curve must undergo a transition to a state belonging to the lower branch, in response to certain perturbations. This transition must be accompanied by the release of a tremendous amount of energy from the star, an amount of the order of 10% of the star's intrinsic energy ( $M c^2$ ).

Two questions arise at this point: 1) How large and of what nature must be the perturbation of the state responsible for the star's passing from the upper equilibrium state to the lower. Would an infinitely small perturbation be adequate to produce the result? 2) How

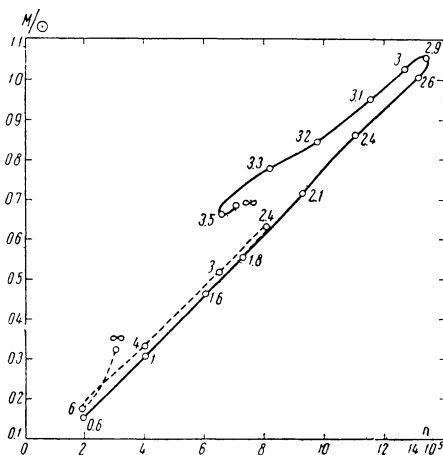


Fig. 5. Dependence of mass of configurations on total number of baryons. Numbers next to circles indicate values of parameter  $t_n$  at the center of the configurations for those points. Solid-line curve refers to real-gas models and dashed-line curve refers to ideal-gas models. The range  $0.6 < t_n(0) \lesssim 1.8$  is traced out in common by both curves.

rapidly the transition will go to completion in the presence of an adequate perturbation.

Both these questions merit special scrutiny. If an infinitely small perturbation is inadequate and the transition requires some finite change in a finite volume, this will mean that the upper states are metastable and may persist for a more or less protracted time interval. It seems quite probable, on the other hand, that the transition process, once initiated, could hardly be contained by any forces. The most likely variant is therefore that the transition is of explosive character. The possibility that the transition discussed is a transition with features of an explosive nature from some metastable state to a perfectly stable state accompanied by the release of an enormous amount of energy seems therefore not at all excluded, in the authors' view.

### 3. Gravitational Mass Defect

With the number of baryons in the star known, we are in a position to calculate the gravitational mass defect, i.e., the quantity

$$\Delta M = n \cdot m_H - M, \quad (3.1)$$

where  $m_H$  is the mass of the hydrogen atom,  $M$  is the mass of the star, and  $n$  is the number of baryons present. We here introduce the notation

$$\frac{\Delta M_1}{n \cdot m_H} \equiv \alpha_1 \quad (3.2)$$

and term this quantity the packing fraction. Results of computations for configurations of an ideal and of a real gas are entered in the fifth and eleventh columns of Table 1.

In contrast to the  $M$  mass values, the computed  $\alpha_1$  values do not vary at all smoothly enough. The reason for this resides in the errors which inevitably plague calculations of Eq. (3.1). For certain reasons (we incur errors in computing both  $M$  and  $n$ ) the relative error comes out quite large in this case.

A survey of  $\alpha_1$  values listed in Table 1 demonstrates that the configuration associated with  $t_n(0) \leq 2.4$  is absolutely stable in the case of an ideal gas, while the configuration associated with  $t_n(0) \leq 2.9$  is absolutely stable in the case of a real gas. The remaining configurations are either metastable or unstable. There is one intriguing feature in the unstable branches, namely that for  $t_n(0) \gtrsim 4.2$  in the case of an ideal gas and for  $t_n(0) \gtrsim 3.15$  in the case of a real gas, the binding energy  $\Delta M_1$  has a negative value. This is related to the fact that the mass intrinsic to hyperons exceeds the mass of nucleons, while at the same time the gas will consist entirely of nucleons (protons and electrons, to be exact) when it is scattered. It is not excluded that configurations having a negative  $\Delta M_1$  value may exist in nature, but such states will be less stable than the others. In response to external disturbances, such configurations would eventually go over into a stable state correspond-

ing to the upper branch of the  $\alpha_1(n)$  curve (to which the lower branch of the curve plotted in Fig. 5 corresponds). A tremendous quantity of energy would have to be explosively liberated in the process.

In including this section, let us consider another gravitational mass defect,  $\Delta M_2 = M_0 - M$ , where

$$M_0 = \frac{4\pi}{c^2} \int_0^R \sqrt{g_{rr}} \cdot r^2 \rho(r) dr. \quad (3.3)$$

$\Delta M_2$  shall be termed the macroscopic mass defect. Let us also introduce the concept of a macroscopic packing fraction

$$\frac{\Delta M_2}{M} \equiv \alpha_2. \quad (3.4)$$

$\alpha_2$  is thus the mass defect referred to a unit mass of a degenerate Fermi baryon gas.

Values of  $\alpha_2$  were obtained by D. Sedrakyan, a student at the University of Erevan. The results are listed in the sixth and twelfth columns of Table 1. As we readily see, the mass defect  $\Delta M_2$  for the configurations in question is quite large. For the densest configurations, this mass is of the same order of magnitude as the mass of the star itself.

### 4. On Extremely High Densities of Matter

Above, we undertook a formal treatment of the case of infinitely high density. However, the problem of the state of matter in such cases where the mean distances between particles become appreciably smaller than the radius of the pion cloud surrounding the baryons (1.4 fermi) is still an open question.

If the cores are identical in all the baryons or at least in some of them, additional forces of a repulsive nature must make themselves felt as soon as particles execute close approaches, as was quite correctly noted by Zel'dovich [4] in line with the Pauli principle. Taking this to be a valid assumption, the theory of a superdense degenerate state as presented in our first contribution [5] can no longer be considered applicable for the range  $N \gtrsim 10^{41} \text{ cm}^{-3}$  ( $t_n > 4.8$ ).

In order to describe the state of matter at such densities, it seems that we must entertain new physical concepts. Without laying claim to even a rough tentative solution to the problem, we should like to point out several important possibilities.

When the density of matter increases the pion clouds of neighboring particles deform each other. At a reasonably high density we can no longer speak of separate pion clouds surrounding individual cores. The totality of the cores is found in a continuous pion field. If the cores of all types of baryons are identical, we must speak in essence of a degenerate gas of cores, i.e., of a degenerate gas consisting of heavy particles of one type and a small quantity of  $\pi$ -mesons.

There perhaps exist two or several different types of cores. That is, let us postulate the existence of neutral and positively charged cores, to be denoted  $Y^0$  and  $Y^+$ . Let us further assume half-integral spin for each of these variants.

In that case, electrons,  $\mu^-$ - and  $\pi^-$ -mesons are suitable candidates as stable components of matter in addition to those two core types. In a manner similar to that followed in the preceding contribution, we may find the state of such a gas from a corresponding variational principle, by assigning a total number of cores and observing the neutrality condition. As a result, we derive the equilibrium condition:

$$E_{Y^+} + m_\pi c^2 = E_{Y^0}, \quad (4.1)$$

$$E_e = E_\mu = m_\pi \cdot c^2, \quad (4.2)$$

where the subscripted E's indicate the cutoff energy of the appropriate particles. From Eq. (4.1), we have

$$m_+ \cosh(t_+/4) = m_0 \cdot \cosh(t_0/4) - m_\pi, \quad (4.3)$$

and from Eq. (4.2) we have

$$N_k = \begin{cases} 1.20 \cdot 10^{37} \text{ cm}^{-3} & \text{at } k = e, \\ 3.38 \cdot 10^{36} \text{ cm}^{-3} & \text{at } k = \mu. \end{cases} \quad (4.4)$$

The concentration of  $\pi^-$ -mesons is found from the neutrality conditions

$$N_\pi = N^+ - N_e - N_\mu. \quad (4.5)$$

Since the concentrations of electrons and  $\mu^-$ -mesons must be much smaller than the concentration of other remaining particles, we may state that

$$N_\pi \approx N^+ \approx N^0.$$

Returning to the assumption that there exists only one type of core, let us take note of two possible variants applicable in this case. If this unique core is neutral, matter cannot exist in the form of any other kind of elementary particle.

If on the other hand the core is of positive charge for all baryons, then electrons,  $\pi^-$ - and  $\mu^-$ -mesons are capable of existence in addition to cores. In a state of thermodynamical equilibrium we have

$$E_e = E_\mu = m_\pi c^2. \quad (4.6)$$

Finally, the neutrality condition yields for the baryon concentration

$$N_Y = N_\pi + N_e + N_\mu \approx N_\pi. \quad (4.7)$$

Further consideration of these problems would confront us with many confusing and puzzling aspects. We shall therefore rest our case at this point, the more so

inasmuch as the introduction of matter consisting of cores can obviously have no effect on the order of magnitude of the mass of equilibrium configurations.

### Summary

The investigation of the internal structure of superdense configurations consisting of highly degenerate baryon gas demonstrates that the metric must deviate strongly from the Euclidean metric in the interior of a star and in the regions of space immediately surrounding the star. We must therefore always accept Einstein's theory of gravitation as the point of departure in calculating hyperon star configurations.

The basic feature of each configuration is the number of baryons  $\underline{n}$  in a star. However, it is found that two or three equilibrium configurations with different mass values correspond to several values of  $\underline{n}$ . Of these, the configuration associated with the least mass value will be the most stable. The question of a possible metastable state of higher energy was posed. A study of the process of transition from higher-energy to lower-energy states was also seen to be of interest.

The authors express their acknowledgment to G. S. Sargsyan and N. G. Akopyan for their work in performing the numerical computations.

### LITERATURE CITED

1. V. A. Ambartsumyan and G. S. Saakyan, *Astron. zhur.*, **38**, 785 (1961), [*Soviet Astron. - AJ*, Vol. 5, p. 601].
2. J. R. Oppenheimer and G. M. Volkoff, *Phys. Rev.*, **55**, 374 (1939).
3. L. Landau and E. Lifshits, *Statistical Physics* [in Russian] (Gostekhizdat, 1951) [English translation, Addison Wesley].
4. Ya. B. Zel'dovich, *Zhur. eksptl. i teoret. fiz.*, **37**, 569 (1959); [*Soviet Physics - JETP*, Vol. 10, p. 403].
5. V. A. Ambartsumyan and G. S. Saakyan, *Astron. zhur.*, **37**, 193 (1960), [*Soviet Astron. - AJ*, Vol. 4, p. 187].

All abbreviations of periodicals in the above bibliography are letter-by-letter transliterations of the abbreviations as given in the original Russian journal. *Some or all of this periodical literature may well be available in English translation.* A complete list of the cover-to-cover English translations appears at the back of this issue.